Epoxy Resin Modified with *In Situ* Generated Metal Oxides by Means of Sol–Gel Process

Federica Bondioli,[1] Maria Elena Darecchio,[1] Adrian S. Luyt,[2] Massimo Messori[1]

[1]*Dipartimento di Ingegneria dei Materiali e dell'Ambiente, Università di Modena e Reggio Emilia, Via Vignolese 905/A, 41125 Modena, Italy*
[2]*Department of Chemistry, University of the Free State (Qwaqwa Campus), Phuthaditjhaba 9866, South Africa*

Received 2 December 2010; accepted 25 January 2011
DOI 10.1002/app.34264
Published online 10 June 2011 in Wiley Online Library (wileyonlinelibrary.com).

ABSTRACT: Organic–inorganic hybrids were prepared with silica, zirconia, or titania *in situ* generated within epoxy resins based on bisphenol A diglycidyl ether and Jeffamine® by means of the aqueous sol–gel process. The morphology of the prepared hybrids varied from a particulate dispersed phase to a co-continuous morphology. Silica and zirconia filled epoxies were characterized by a significant increase in thermal stability, attributable to the high thermal stability of silica and zirconia phases. On the contrary, the introduction of titania induced a strong decrease in thermal stability of the epoxy/titania hybrids compared with the pure epoxy resin, attributable to metal-catalyzed oxidative decomposition mechanism in the polymer/titania composite. Hybrids were much more transparent than unfilled epoxy. The transmittance of silica- and titania-based hybrids showed a slight decrease by increasing the content of filler, while the transparency of zirconia-based hybrids was very high and almost constant independently by the nominal content of filler. The presence of *in situ* generated fillers significantly enhanced the scratch resistance of the epoxy resin as indicated by the marked increase of critical load for all the hybrids. © 2011 Wiley Periodicals, Inc. J Appl Polym Sci 122: 1792–1799, 2011

Key words: thermosets; composites; fillers

INTRODUCTION

Epoxy resins represent a class of thermosetting polymers widely used in the field of adhesives, potting compounds, molding compounds, and in the fabrication of fiber-reinforced polymer matrix composites for structural applications. Epoxies present several advantages over other types of polymers, such as inherently polar nature that results in outstanding adhesion to a wide variety of substrates, relatively low cure shrinkage that makes dimensional stability, no volatile by-products of the curing reaction, and crosslinked structure that confers excellent resistance to aggressive environments. Furthermore, epoxies have remarkable versatility because of the possibility to be formulated to meet a broad range of specific processing and performance needs.[1]

The improvement of the mechanical properties (reinforcement) of epoxy resins by addition of rigid fillers represents an important aspect in the field of polymer science and technology. The interactions between epoxy matrix and filler, which can be increased if good dispersion and distribution of the particulate are achieved, play a fundamental role for the increase of mechanical properties. The surface characteristics of the particles (presence of reactive/functional groups, wettability, and surface energy) and the chemical nature of the polymer represent the key parameters for these interactions.

Concerning the field of fillers having dimensions in the nanometric scale, polymer matrix nanocomposites have attracted extraordinary attention in the last decade on the basis of their excellent mechanical and barrier properties compared with the conventional microcomposites, usually at very low filler content. Layered silicates, ceramic nanoparticles (such as silica, titania, and zirconia), carbon nanofibers, and nanotubes are typical examples of materials used as nanosize reinforcing additives.[2]

The usual method for the preparation of nanocomposites is based on the top–down approach according to which preformed nano-objects are dispersed within the polymeric matrix by physical–mechanical mixing. Even if very attracting from an industrial point of view, this method presents some severe limitations related to the difficulties to obtain an

Correspondence to: M. Messori (massimo.messori@unimore.it).

Contract grant sponsor: The South African National Research Foundation; contract grant numbers: GUN62693, GUN65143.
Contract grant sponsor: University of the Free State.
Contract grant sponsor: Italian Ministry of Foreign Affairs.

effective dispersion because of the strong tendency to particles aggregation phenomena and the significant increase of melt viscosity because of the complex rheology of nanocomposite systems.

To minimize these problems and alternatively to the conventional mechanical mixing for the preparation of filled epoxies, the *in situ* generation of inorganic oxides by using the sol–gel process has been recognized as a novel and interesting technique for the preparation of composites.

The classical aqueous (or nonhydrolytic) sol–gel process[3] consists of a two-step hydrolysis–condensation reaction starting with metal alkoxides $M(OR)_x$, according to the following scheme:

Step 1: Hydrolysis

$$M(OR)_x + n\ H_2O \rightarrow M(OR)_{x-n}(OH)_n + n\ ROH$$

Step 2: Condensation

$$\equiv M{-}OH + HO{-}M\equiv \rightarrow \equiv M{-}O{-}M\equiv + H_2O$$

(water condensation)

and/or

$$\equiv M{-}OR + HO{-}M\equiv \rightarrow \equiv M{-}O{-}M\equiv + ROH$$

(alcohol condensation).

The presence in the reactive system of an organic oligomer or polymer leads to the formation of organic–inorganic hybrid structures composed of metal oxide and organic phases intimately mixed each other. This synthetic procedure belongs to the so-called "bottom–up" approach for the preparation of hybrid materials and, depending on the experimental conditions, permits the synthesis of composite structures in which the dimensions of the dispersed phase are under 100 nm (nanocomposites). The optical, physical, and mechanical properties of these nanocomposites are strongly dependent not only on the individual properties of each component but also on important aspects of the chemistry involved such as uniformity, phase continuity, domain size, and the molecular mixing at the phase boundaries.

Concerning the synthesis and characterization of epoxy–silica hybrids prepared by the sol–gel process, Matejka and coworkers published several papers on this topic. Diglycidyl ether of bisphenol A (DGEBA) and Jeffamine® polyoxyalkyleneamines were generally used as epoxy and amine hardener, respectively. Silica particles were *in situ* generated starting from tetraethoxysilane (TEOS) in the presence of water and in acidic conditions in three different synthetic ways: (i) one-step procedure (all reaction components were mixed and reacted together), (ii) two-step procedure with prehydrolyzed TEOS (TEOS were prehydrolyzed and subsequently added to DGEBA and Jeffamine®), and (iii) two-step procedure with preformed epoxy network (TEOS were swollen and reacted within a cured DGEBA-Jeffamine® system).[4,5] Authors found that kinetics of the silica structure build-up in the organic matrix, its final structure, and morphology depend on the method of hybrid preparation. The large compact silica aggregates (diameter 100–300 nm) are formed during the one-stage procedure. The two-stage procedure with the acid prehydrolysis of TEOS leads to an acceleration of gelation and formation of more open and smaller silica structures (diameter 50–100 nm). The most homogeneous hybrid morphology (with the smallest silica domains of size 10–20 nm) appears in the two-step procedure with preformed epoxy network presumably because of the fact that the development of the silica structure is restricted by a rigid reaction medium of the preformed epoxy network. Concerning mechanical properties, the rubbery epoxy network DGEBA-Jeffamine® was reinforced with silica formed *in situ*, and an increase in the modulus by two orders of magnitude at low contents of the silica phase (10 vol %) was observed.[6] Matejka and coworkers presented a more recent article dealing with the preparation and characterization of hybrid organic–inorganic epoxy-based films and coatings obtained by replacing the conventional DGEBA resin with different trialkoxysilanes having epoxy functionalities and by using Jeffamine® polyoxyalkyleneamines having different molecular weights as hardeners.[7] The structure evolution during the network formation and the surface morphology were deeply studied as a function of reaction conditions and molecular structures of the reactants.

Macan et al. prepared and characterized organic–inorganic hybrid materials based on DGEBA and 3-glycidyloxypropyltrimethoxysilane (GPTMS) and using a Jeffamine® poly(oxypropylene) amine as a curing agent.[8,9] GPTMS was the precursor of silica phase through absorption of the air humidity for the sol–gel process. Total conversion of epoxy groups was found to decrease with increasing content of GPTMS and is attributed to sterical hindrance of inorganic phase. The presence of a silica phase also immobilizes the organic chains and improves the temperature stability of hybrid materials.

In a very similar way, Ochi and coworkers prepared several kinds of epoxy–silica hybrids from DGEBA, primary or tertiary amines as hardener, and GPTMS or tetramethoxysilane (TMOS) as silica precursor.[10–12] In the hybrids containing GPTMS and cured with primary amines, the storage modulus in the rubbery region increased and the peak area of the tanδ curves in the glass transition region decreased with the hybridization of small amounts of silica. Authors exploited this behavior as a suppression of the epoxy network moiety with the incorporation of a silica network containing a functional (epoxy) group that can react with the organic component. The prepared hybrids were also

proposed as adhesives, and the GPTMS-based hybrids showed a very high bonding strength for the silicone rubber compared with that of the unmodified epoxy resin, but this improvement in the bonding strength was not observed in the hybrids with TMOS. The high bonding strength observed in the DGEBA/GPTMS hybrids was due to the formation of the interfacial bonding between the silica networks formed on the substrate surface and the epoxy networks in the adhesive layer. Recently, a novel adhesive based on the combination of DGEBA/sol–gel system and nanofillers, such as alumina or carbon nanotubes, has also been proposed by Akid and coworkers.[13]

Turri et al. presented a very recent article on abrasion and scratch resistance of nanostructured epoxy coating.[14] Authors prepared a series of epoxy nanostructured coatings based on DGEBA and an isophorone diamine hardener. Top–down nanocomposites were obtained by the mechanical dispersion of nanoalumina, silanized nanoalumina, and organomodified clays. On the contrary, bottom–up hybrids were achieved after the silanization of the DGEBA resin and after cocrosslinking with TEOS through a self-catalyzed sol–gel process. Results indicated that, in the top–down nanocomposites, there were minor changes in the surface hardness and a slight improvement in the abrasion resistance, whereas the nanoscratch resistance assessed by AFM tests showed significantly better performances in the hybrid coatings obtained through sol–gel chemistry.

Jeng and coworkers prepared phenolic novolac/SiO_2 and cresol novolac epoxy/SiO_2 hybrids through *in situ* sol–gel reaction of TEOS. The formed hybrids were used as a curing agent and as epoxy resin in epoxy curing compositions, respectively. High glass transition temperatures, outstanding thermal stability, enhanced flame retardance, and low coefficient of thermal expansion were observed for the cured epoxy/silica samples.[15]

Other than silica, also titania and zirconia have been proposed as *in situ* generated inorganic phases for the modification of epoxy resins. Silica–titania mixed oxides were *in situ* generated in DGEBA, which was then cured with 4,4′-diaminodiphenylsulphone[16] or in cycloaliphatic epoxy acrylate oligomers[17] for UV-curable coatings. Epoxy/titania hybrids for nanoimprint lithography were prepared by mixing and reacting DGEBA, tetraethyl orthotitanate (TEOT), and acetylacetone in the presence of GPTMS as coupling agent. The curing of the epoxy/titania precursor was carried out by adding an aliphatic amine.[18]

Completely transparent polymeric films based on photocured epoxy networks containing TiO_2 nanoparticles were prepared by Sangermano et al.[19] by their *in situ* generation via sol–gel process in the presence of GPTMS as coupling agent. Authors showed that by increasing the TiO_2 concentration, a decrease in the rate of polymerization and epoxy group conversion was induced because of the UV adsorption competition of TiO_2 nanoparticles and the photoinitiator.

The preparation of high refractive index epoxy/TiO_2 nanocomposite for optical antirefractive films has also been reported by Yang and coworkers[20] who demonstrated that the refractive index of these materials can be continuously adjusted from 1.61 to 1.797 with the content of TiO_2 increasing from 0 to 65 wt %. Transparent hydrophilic epoxy/TiO_2 nanocomposites were prepared from tetrabutyl titanate.[21]

Ochi et al. also reported the synthesis of epoxy/zirconia hybrid materials from DGEBA, zirconium tetra-*n*-propoxide, and acetic acid via *in situ* polymerization.[22] As a result, ZrO_2 produced by sol–gel was uniformly dispersed into the epoxy matrix at a nanoscale or less, and the hybrid materials exhibited an excellent optical transparency and refractive indices significantly improved with the increasing zirconia contents (1.621 at 18.4 wt %). Concerning mechanical properties, with the increasing zirconia contents, the storage modulus in the high temperature region increased, and the glass transition temperature of the hybrid materials shifted to a higher temperature.

Sangermano et al.[23] reported the preparation of nanostructured organic–inorganic hybrid epoxy coatings containing zirconia domains obtained via a cationic UV/thermal dual-cure process. The UV-cured films showed an increase in the refractive index by increasing the zirconia precursor content in the photocurable formulation, reaching the value 1.580 in the presence of 5 wt % of zirconium tetrapropoxide.

To compare the effect of different *in situ* generated fillers, the present article deals with the preparation and characterization of epoxy resins modified with silica, zirconia, or titania particles by means of the aqueous sol–gel process. Particular attention was devoted on their thermal stability and scratch resistance properties because of a lack of these important parameters in the published literature.

EXPERIMENTAL

Materials

Bisphenol A diglycidyl ether (D.E.R.® 332, Midland, Michigan for Dow Chemicals Co.) with a maximum epoxide equivalent weight of 178 g mol^{-1} was purchased from Sigma-Aldrich (Milano, Italy).

Poly(propylene glycol)-*b*-poly(ethylene glycol)-*b*-poly(propylene glycol) bis(2-aminopropyl ether) (Jeffamine® J1900, The Woodlands, Texas for Huntsman Petrochemical Corp.) with an average M_n of

about 1900 g mol^{-1} was purchased from Sigma-Aldrich (Milano, Italy).

The molecular structures of D.E.R.® 332 and Jeffamine® J1900 are reported as follows:

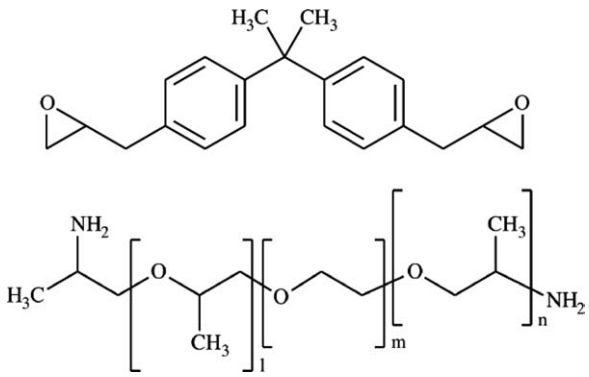

Tetraethoxysilane (TEOS), titanium *iso*-propoxide (TIP), zirconium *iso*-propoxide (ZIP), acetylacetone, ethanol, and dibutyltin oxide (DBTO) were purchased from Sigma-Aldrich (Milano, Italy).

All materials were used as received without any further purification.

Preparation of hybrid materials

For the preparation of epoxy resins modified with *in situ* generated silica, TEOS, water, ethanol, and DBTO (molar ratio 1 : 4 : 4 : 0.01) were mixed at room temperature for about 10 min.

For the preparation of epoxy resins modified with *in situ* generated titania and zirconia, taking into account the much higher reactivity of titania and zirconia alkoxides with respect to TEOS, TIP, and ZIP were prereacted with acetylacetone as bidentate complexing ligand to decrease their reactivity.[24] Furthermore, water was not added directly to the reactive mixture, but it was absorbed from the external humid atmosphere in the absence of a sol–gel catalyst. TIP or ZIP were mixed with acetylacetone (molar ratio 1 : 1) at room temperature for about 40 min.

In all cases, the sol–gel system was subsequently added and mixed to Jeffamine® J1900 until a homogeneous solution was obtained. The solution was then mixed to D.E.R.® 332, and the liquid was cast in suitable silicone molds or manually roll-coated onto PC slabs. The materials were maintained for 24 h at room temperature and subsequently postcured for 4 h at 170°C.

Jeffamine® J1900 and D.E.R.® 332 were mixed at a stoichiometric ratio. TEOS, TIP, or ZIP amount was varied to obtain a nominal metal oxide content (i.e., by assuming the completion of the sol–gel reaction of metal alkoxide to metal oxide) of 10, 30, and 50 phr, respectively. Code and composition of the prepared materials are reported in Table I.

TABLE I
Code and Nominal and Actual Composition of the Prepared Materials

Material code	Type of filler	Nominal filler content (phr)	Nominal filler content (wt %)	Actual filler content[a] (wt %)
Ep	None	0	0	0.0 (-)
Ep/SiO_2 10	SiO_2	10	9.1	11.8 (130%)
Ep/SiO_2 30	SiO_2	30	23.1	22.7 (98%)
Ep/SiO_2 50	SiO_2	50	33.3	30.8 (93%)
Ep/TiO_2 10	TiO_2	10	9.1	7.3 (80%)
Ep/TiO_2 30	TiO_2	30	23.1	19.1 (83%)
Ep/TiO_2 50	TiO_2	50	33.3	28.0 (84%)
Ep/ZrO_2 10	ZrO_2	10	9.1	6.8 (75%)
Ep/ZrO_2 30	ZrO_2	30	23.1	13.8 (60%)
Ep/ZrO_2 50	ZrO_2	50	33.3	22.0 (66%)

[a] Determined by TGA (in air, residue at 700°C). In bracket, the conversion of metal alkoxide to metal oxide with respect to the nominal value is reported.

Characterization

The morphological investigation was carried out using a scanning electron microscope (SEM, Quanta 200, FEI, USA) by applying an accelerating voltage of 15 kV. The sample surfaces (cross sections) were coated with gold by an electrodeposition method to impart electrical conduction before recording SEM micrographs.

Thermogravimetric (TG) analysis was carried out on a Perkin–Elmer TGA7 Thermogravimetric Analyzer under air flow, at a heating rate of 20°C min^{-1} and up to 700°C.

Transparency of hybrid films applied onto microscope glasses by roll-coating (films thickness of about 80 μm) was characterized by UV–Vis spectrophotometry (Perkin–Elmer, Lambda 19) in the 400–800 nm range.

Scratch tests were carried out on a CSM Micro-Combi Tester by using a Rockwell C diamond scratch indenter (tip radius $R = 200$ μm) and by progressively increasing the load from 0.1*N* to 20*N* at a load rate of 6.6*N* min^{-1} for a scratch length of 3 mm. This kind of scratch indenter was chosen to produce a sharp scratch on the surfaces. A prescan with a very small load was carried out, during which the starting surface profile was measured and subtracted from the loaded scratch scan profile to determine the depth of surface penetration (penetration depth, *Pd*). The instrument was equipped with an integrated optical microscope. Three scratches were carried out in different areas for each specimen, and averaged values of the load at which the scratch track appears (first critical load, Lc_1) were determined by optical methods for each analysis.

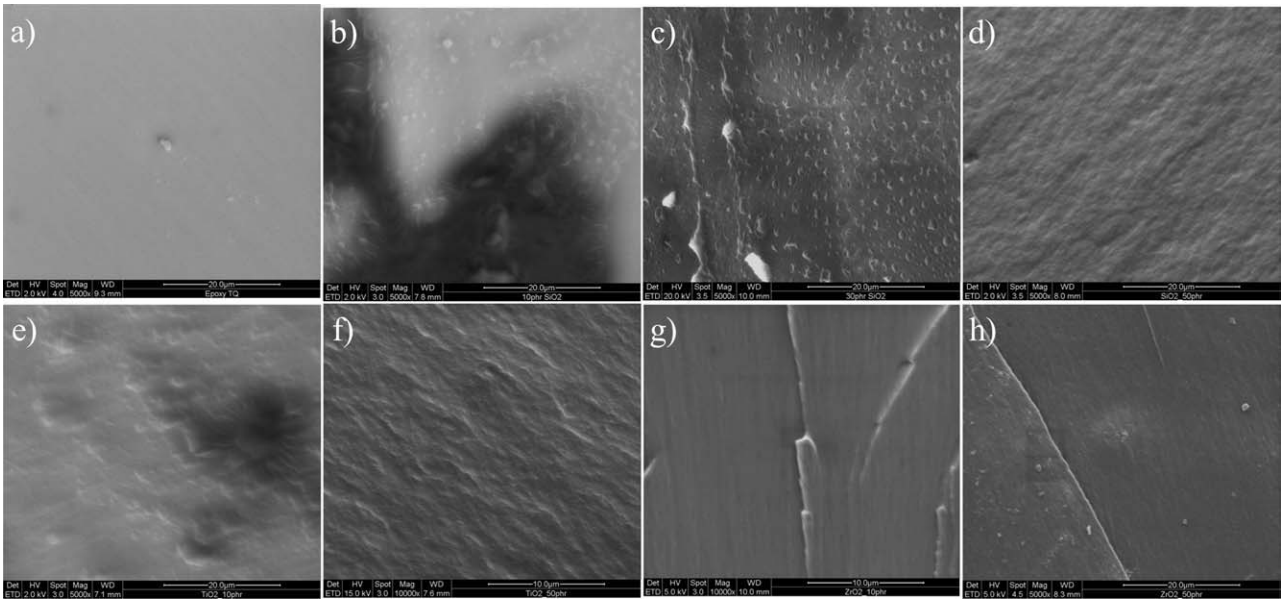

Figure 1 SEM micrographs of the fracture surface of (a) "Ep," (b) "Ep/SiO_2 10," (c) "Ep/SiO_2 30," (d) "Ep/SiO_2 50," (e) "Ep/TiO_2 10," (f) "Ep/TiO_2 50," (g) "Ep/ZrO_2 10," and (h) "Ep/ZrO_2 50."

RESULTS AND DISCUSSION

Morphological characterization

SEM images of fracture surface of the prepared materials are reported in Figure 1. As expected, the fracture surface of "Ep" was very smooth and uniform according to the homogeneous nature of the unfilled epoxy [Fig. 1(a)]. On the contrary, silica-based hybrids with a nominal filler content of 10 and 30 phr revealed the presence of a distinct dispersed phase having submicrometer dimensions and attributable to silica particles (the silica nature of this dispersed phase was also confirmed by SEM images collected with backscattered electrons and by EDS analysis). Quite interestingly, the presence of a dispersed phase was not evident at the highest magnification in the case of "Ep/SiO_2 50" for which a rough but chemically homogeneous surface was shown [Fig. 1(d)]. The disappearing of a particulate morphology by increasing the silica content could be tentatively attributed to the shift from a dispersed morphology to a co-continuous one as already evidenced for very similar materials by Matejka and coworkers, which demonstrated that the hybrid system did not correspond to the morphological model of a particulate composite consisting of epoxy matrix and dispersed rigid silica particles. In particular, authors showed that dynamic mechanical properties fit the model assuming the co-continuous morphology of the epoxy matrix and of the silica phase or the silica–glassy epoxide phase continuously extending through the macroscopic sample.[6]

A very similar morphology was shown by titania-based hybrids for which the presence of dispersed titania particles was evident only at low filler content ["Ep/TiO_2 10," Fig. 1(e)], while a homogeneous surface was formed at higher titania content ["Ep/TiO_2 50," Fig. 1(f)].

A significantly different behavior was shown by zirconia-based hybrids for which a very smooth and uniform fracture surface was present at low zirconia content ["Ep/ZrO_2 10," Fig. 1(g)], while a particulate phase was visible at highest zirconia content ["Ep/ZrO_2 50," Fig. 1(h)]. In this case, the absence of a dispersed phase at low filler concentration could be presumably attributed to the nanometric dimensions of zirconia particles, not detectable by SEM analysis.

Thermal stability

TG analysis was used to determine the actual content of metal oxide and to investigate the thermal oxidative stability of these organic–inorganic hybrid materials.

The actual filler content values are reported in Table I. In the case of silica-based hybrids, the actual filler contents were very near to the expected values, indicating that the experimental conditions used were appropriate to induce an almost complete conversion of TEOS to silica. On the contrary, the actual filler contents determined for titania- and zirconia-based hybrids were significantly lower than the expected values with conversions of TIP to titania in the range 80%–84% and of ZIP to zirconia in the range 60%–75%. It can be assumed that the presence of acetylacetone as bidentate complexing ligand for TIP and ZIP and the absence of directly added water and catalysts decreased significantly the reactivity of

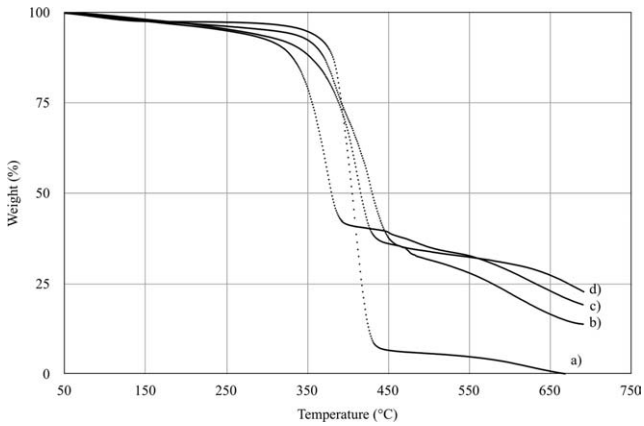

Figure 2 Thermograms of (a) "Ep," (b) "Ep/ZrO_2 30," (c) "Ep/TiO_2 30," and (d) "Ep/SiO_2 30" in the temperature range 50–700°C.

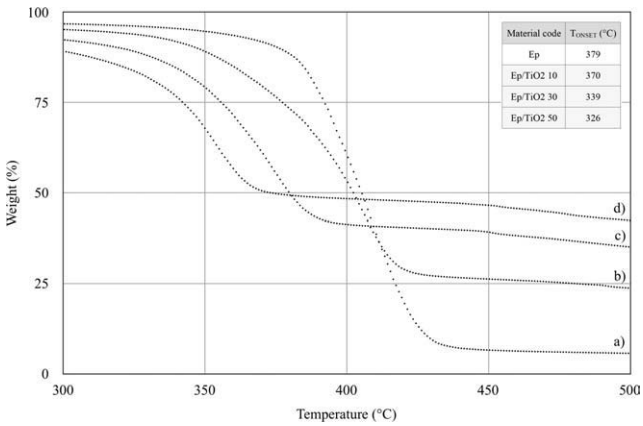

Figure 4 Thermograms of (a) "Ep," (b) "Ep/TiO_2 10," (c) "Ep/TiO_2 30," and (d) "Ep/TiO_2 50" in the temperature range 300–500°C.

the titania and zirconia alkoxides and limited their complete conversion to the respective oxides.

Representative thermograms of epoxy resin "Ep" and of hybrids having a nominal filler content of 30 phr are reported in Figure 2. It is possible to see that the weight losses of all the samples occurred in three distinct steps. In the first step, the weight loss at around 100–250°C was probably due to the evaporation of strongly absorbed water and condensation by-products of metal alkoxide compounds. The second step corresponding to the maximum weight loss in the range of 300–450°C was ascribed to the decomposition of the polymer chain. In the third step, the weight loss at around 450–700°C was presumably due to the combustion of char residues formed in the previous step.

The onset temperature (T_{ONSET}) values of the degradation step in the temperature range 300–450°C (degradation of the organic polymer network) are reported in Figures 3–5. T_{ONSET} data for silica- and zirconia-filled epoxy resins were substantially unchanged with respect to the value of pure epoxy (379°C), while, on the contrary, the presence of titania within the organic polymer led to a significant decrease of the onset temperatures with values which decrease by increasing the filler content reaching the minimum value of 326°C for "Ep/TiO_2 50." Apart the onset temperature values, a more detailed analysis of the thermal-oxidative behavior can be made examining Figures 3–5, which report the thermogram expansion in the temperature range 300–500°C for all three series of samples.

It is evident that in the case of "Ep/SiO_2" and "Ep/ZrO_2" materials, the onset temperature was not fully appropriate to describe the thermal stability, because it is strongly influenced by the different slopes of the thermograms of different materials. As said earlier, T_{ONSET} values for silica- and zirconia-filled epoxy resins were very near to that of pure epoxy. With respect to pure epoxy, thermogram traces of silica- and zirconia-filled epoxies (Figs. 3 and 5) indicated that the degradation process, even if slightly anticipated at lower temperatures, continued until to much higher temperatures indicating a

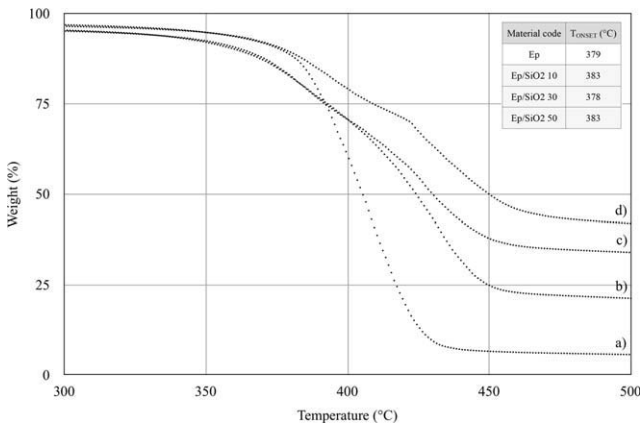

Figure 3 Thermograms of (a) "Ep," (b) "Ep/SiO_2 10," (c) "Ep/SiO_2 30," and (d) "Ep/SiO_2 50" in the temperature range 300–500°C.

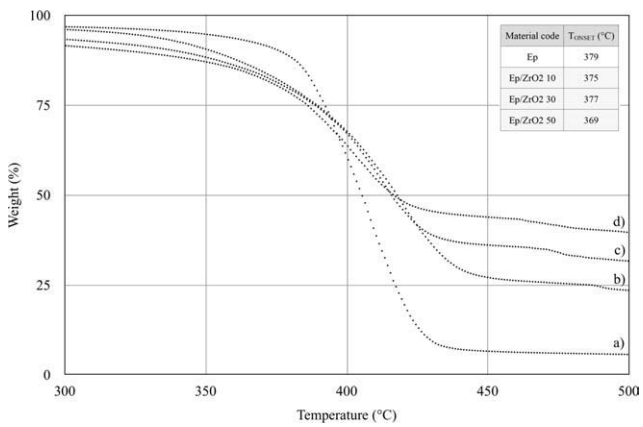

Figure 5 Thermograms of (a) "Ep," (b) "Ep/ZrO_2 10," (c) "Ep/ZrO_2 30," and (d) "Ep/ZrO_2 50" in the temperature range 300–500°C.

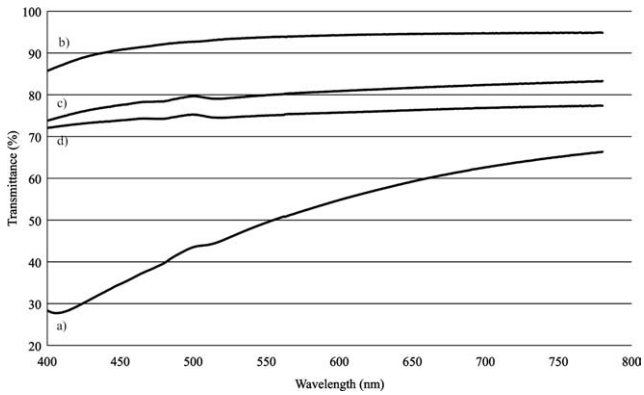

Figure 6 UV–Vis spectra of (a) "Ep," (b) "Ep/SiO_2 10," (c) "Ep/SiO_2 30," and (d) "Ep/SiO_2 50."

significant increase in thermal stability, which could be attributed to the high thermal stability of silica and zirconia phases. On the other hand, the thermogram traces of "Ep/TiO_2" samples were clearly shifted toward lower temperatures by an extent which increased by increasing the titania content according to the already discussed T_{ONSET} data and confirming that the introduction of titania caused a strong decrease in thermal stability of the epoxy/titania hybrids compared with the pure epoxy resin. The dramatic decrease in thermal stability could probably be attributed to metal-catalyzed oxidative decomposition pathways in the polymer/titania composite, as already observed and discussed for similar materials.[18]

Optical properties-transparency

Transparency of thin films can represent a key parameter for the use of the present hybrids as coatings. Transparency of hybrid films applied onto microscope glasses having comparable thickness values (about 80 μm) was evaluated by means of UV–Vis spectrophotometry. The UV–Vis spectra of the investigated hybrids are reported in Figures 6–8.

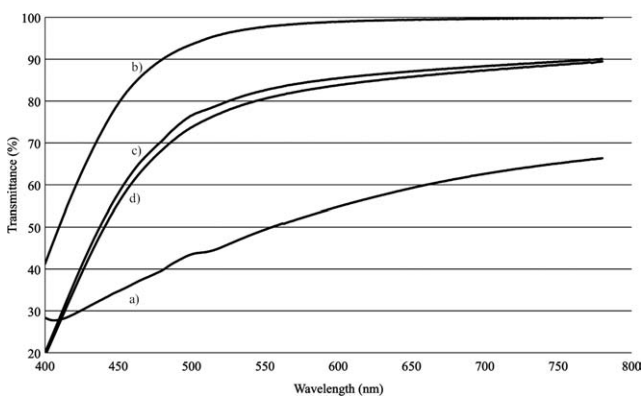

Figure 7 UV–Vis spectra of (a) "Ep," (b) "Ep/TiO_2 10," (c) "Ep/TiO_2 30," and (d) "Ep/TiO_2 50."

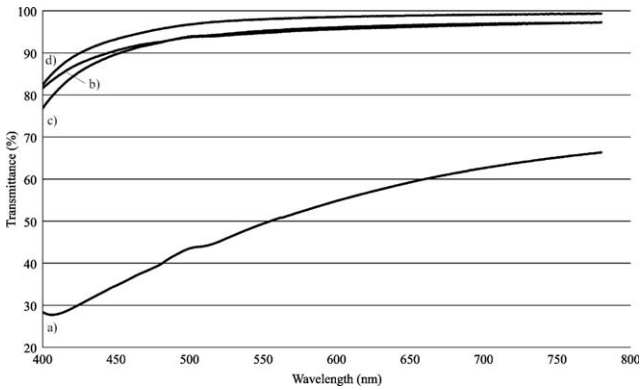

Figure 8 UV–Vis spectra of (a) "Ep," (b) "Ep/ZrO_2 10," (c) "Ep/ZrO_2 30," and (d) "Ep/ZrO_2 50."

Unfilled epoxy "Ep" appeared slightly opaque at a visual inspection, and this limited transparency was confirmed by the relatively low values of transmittance reported. The slight opacity of the sample can be reasonably explained by taking into account the tendency, even limited after crosslinking, to crystallization of Jeffamine® poly(oxypropylene) amine hardener. In this respect, it could be speculated that the filled samples showed a much higher transparency because of the presence of the *in situ* generated inorganic particles, which could act as nucleating agent (decreasing the dimension of crystallites under the wavelength of visible light) or as inhibitors of the crystallization process.

Transmittance values of silica- and titania-based hybrids showed a slight decrease by increasing the content of filler, while the transparency of zirconia-based hybrids was very high and almost constant independently by the nominal content of ZrO_2.

Scratch resistance

The load at which the scratch track appears (first critical load, Lc_1) and penetration depth (Pd) measured at a normal load of 1N are reported in Table II.

TABLE II
Scratch Test: First Critical Load (Lc_1) and Penetration Depth Measured at 1N (Pd_{1N}) of the Prepared Materials

Material code	Lc_1 (N)[a]	Pd_{1N} (μm)[a]
Ep	1.5 (0.4)	9.4 (1.2)
Ep/SiO_2 10	10.3 (6.0)	4.5 (1.0)
Ep/SiO_2 30	11.9 (2.4)	4.2 (0.3)
Ep/SiO_2 50	3.9 (1.9)	4.2 (0.4)
Ep/TiO_2 10	4.3 (0.6)	3.6 (0.6)
Ep/TiO_2 30	6.1 (0.7)	7.5 (4.7)
Ep/TiO_2 50	9.5 (1.3)	9.8 (4.3)
Ep/ZrO_2 10	7.9 (4.4)	5.7 (1.2)
Ep/ZrO_2 30	6.2 (0.4)	4.8 (0.1)
Ep/ZrO_2 50	4.4 (0.3)	4.3 (0.1)

[a] In bracket, the standard deviation is reported.

The highest scratch resistance was shown by silica-based hybrids for which Lc_1 values were higher than 10*N* ("Ep/SiO_2 10" and "Ep/SiO_2 30"), about one order of magnitude higher than that of unfilled epoxy (Lc_1 for "Ep" of 1.5*N*). A significant decrease was observed in the case of the highly filled sample "Ep/SiO_2 50" ($Lc_1 = 3.9N$).

Also, titania- and zirconia-based hybrids showed a significantly increased scratch resistance with respect to "Ep" with highest values of Lc_1 shown by "Ep/TiO_2 50" ($Lc_1 = 9.5N$) and "Ep/ZrO_2 10" ($Lc_1 = 7.9N$), respectively. In these two cases, an opposite trend of scratch resistance as a function of filler content was observed: Lc_1 values increased by increasing the TiO_2 concentration and by decreasing the ZrO_2 concentration, respectively.

Penetration depth (*Pd*) measured before the critical load can be considered as an indication of the film rigidity against indenter penetration. The values of penetration depth detected at 1000 m*N* (Pd_{1N}) are reported in Table II. Similarly to the data described earlier, it was very difficult to find out evident correlations between resistance to penetration, critical load, and filler concentration. For the same applied normal force, silica- and zirconia-based hybrids showed Pd_{1N} values $\sim$ 50% lower than "Ep" ($Pd_{1N} = 9.4$ μm) independently on the SiO_2 or ZrO_2 content. Quite surprisingly, "Ep/TiO_2" series evidenced Pd_{1N} values that increased by increasing the titania content even if a very high standard deviation has to be underlined for these data.

The discussed results confirm that scratch resistance of composite films can be considered as the macroscopic expression of several and complex mechanical phenomena of difficult prediction with several parameters, such as mechanical properties of constitutive materials, interface interaction, film thickness, and materials morphology, playing different and important roles.

CONCLUSIONS

Silica, zirconia, or titania were *in situ* generated within epoxy resins based on bisphenol A diglycidyl ether and Jeffamine® by means of the aqueous sol–gel process. SEM analysis evidenced that the morphology of the prepared hybrids changed from a particulate dispersed phase to a co-continuous morphology. TG analysis showed that silica- and zirconia-filled epoxies were characterized by a significant increase in thermal stability, attributable to the high thermal stability of silica and zirconia phases. On the contrary, the introduction of titania induced a strong decrease in thermal stability of the epoxy/titania hybrids compared with the pure epoxy resin, attributable to metal-catalyzed oxidative decomposition mechanism in the polymer/titania composite. Hybrids were much more transparent than unfilled epoxy. The transmittance of silica- and titania-based hybrids showed a slight decrease by increasing the content of filler, while the transparency of zirconia-based hybrids was very high and almost constant independently by the nominal content of filler. The presence of *in situ* generated fillers significantly enhanced the scratch resistance of the epoxy resin as indicated by the marked increase of critical load for all the hybrids.

References

1. Penn, L. S.; Wang, H. In Handbook of Composites, Second Edition; Peters, S. T., Ed.; Chapman & Hall: London, 1998; Chapter 3.
2. Klein, L. C.; Wojcik, A. B. In Encyclopedia of Materials: Science and Technology; Buschow, K. H., Jr.; Robert, W. C., Merton, C. F., Bernard, I., Edward, J. K., Subhash, M., Patrick, V., Eds.; Elsevier: Oxford, 2001, 7577.
3. Brinker, C.; Scherer, G. Sol-Gel Science: The Physics and Chemistry of Sol-Gel Processing; Academic Press: Boston, 1990.
4. Matejka, L.; Dusek, K.; Plestil, J.; Kriz, J.; Lednicky, F. Polymer 1999, 40, 171.
5. Matejka, L.; Plestil, J.; Dusek, K. J Non-Cryst Solids 1998, 226, 114.
6. Matejka, L.; Dukh, O.; Kolarik, J. Polymer 2000, 41, 1449.
7. Spirkova, M.; Brus, J.; Hlavata, D.; Kamisova, H.; Matejka, L.; Strachota, A. J Appl Polym Sci 2004, 92, 937.
8. Macan, J.; Ivankovic, H.; Ivankovic, M.; Mencer, H. J. J Appl Polym Sci 2004, 92, 498.
9. Macan, J.; Ivankovic, H.; Ivankovic, M.; Mencer, H. J. Thermochim Acta 2004, 414, 219.
10. Ochi, M.; Takahashi, R.; Terauchi, A. Polymer 2001, 42, 5151.
11. Ochi, M.; Takahashi, R. J Polym Sci Polym Phys 2001, 39, 1071.
12. Matsumura, T.; Ochi, M.; Nagata, K. J Appl Polym Sci 2003, 90, 1980.
13. May, M.; Wang, H. M.; Akid, R. Int J Adhes Adhes 2010, 30, 505.
14. Turri, S.; Torlaj, L.; Piccinini, F.; Levi, M. J Appl Polym Sci 2010, 118, 1720.
15. Liu, Y. L.; Lin, Y. L.; Chen, C. P.; Jeng, R. J. J Appl Polym Sci 2003, 90, 4047.
16. Lu, S. R.; Zhang, H. L.; Zhao, C. X.; Wang, X. Y. J Appl Polym Sci 2006, 101, 1075.
17. Karata, S.; Kizilkaya, C.; Kayaman-Apohan, N.; Gungor, A. Prog Org Coat 2007, 60, 140.
18. Wu, C. C.; Hsu, S. L. C. J Phys Chem C 2010, 114, 2179.
19. Sangermano, M.; Malucelli, G.; Amerio, E.; Bongiovanni, R.; Priola, A.; Di Gianni, A.; Voit, B.; Rizza, G. Macromol Mater Eng 2006, 291, 517.
20. Guan, C.; Lu, C. L.; Liu, Y. F.; Yang, B. J Appl Polym Sci 2006, 102, 1631.
21. Sadjadi, M. S.; Farhadyar, N. J Nanosci Nanotechnol 2009, 9, 1172.
22. Ochi, M.; Nii, D.; Suzuki, Y.; Harada, M. J Mater Sci 2010, 45, 2655.
23. Sangermano, M.; Voit, B.; Sordo, F.; Eichhorn, K. J.; Rizza, G. Polymer 2008, 49, 2018.
24. Schubert, U. J Mater Chem 2005, 15, 3701.